

Electronic Supplementary Information

Ionic cocrystals of etiracetam and levetiracetam: the importance of chirality for ionic cocrystals

Lixing Song,[†] Oleksii Shemchuk,[‡] Koen Robeyns,[†] Dario Braga,[‡] Fabrizia Grepioni,^{‡*} Tom Leyssens^{†*}

[†]Institute of Condensed Matter and Nanosciences, Université Catholique de Louvain, Place Louis Pasteur 1, B-1348 Louvain-La-Neuve, Belgium;

[‡]Dipartimento di Chimica “Giacomo Ciamician”, Università di Bologna, Via Selmi 2, 40126 Bologna, Italy *fabrizia.grepioni@unibo.it, *tom.leyssens@uclouvain.be

Hot Stage Microscopy experiment

According to VT-XRPD measurements on crystalline powder of $\text{LEV}_2\cdot\text{CaCl}_2\cdot 2\text{H}_2\text{O}$, a possible recrystallization of the anhydrous form could occur at 250°C ; therefore we tried to obtain single crystals of anhydrous $\text{LEV}_2\cdot\text{CaCl}_2$ by heating the hydrated ICC $\text{LEV}_2\cdot\text{CaCl}_2\cdot 2\text{H}_2\text{O}$ in a Hot Stage Microscopy experiment (HSM) conducted immersing the powder in Fomblin®, a synthetic lubricant composed of carbon, oxygen and fluorine that remains liquid in a very wide range of temperatures (from -100°C to 300°C) and is thermally stable and chemically inert even at very high temperatures. The dehydration process could thus be detected (water bubbles formation) but no crystals could be observed at this temperature; the anhydrous form was then melted, and, after the stage was cooled down to room temperature, a few crystals were recovered of sufficient quality for X-ray structural determination, and they were found to be the hydrated form $\text{LEV}_2\cdot\text{CaCl}_2\cdot 2\text{H}_2\text{O}$.

Superposition information for $\text{LEV}_2\cdot\text{CaCl}_2\cdot 2\text{H}_2\text{O}$ and $\text{ETI}_2\cdot\text{CaCl}_2\cdot 2\text{H}_2\text{O}$.

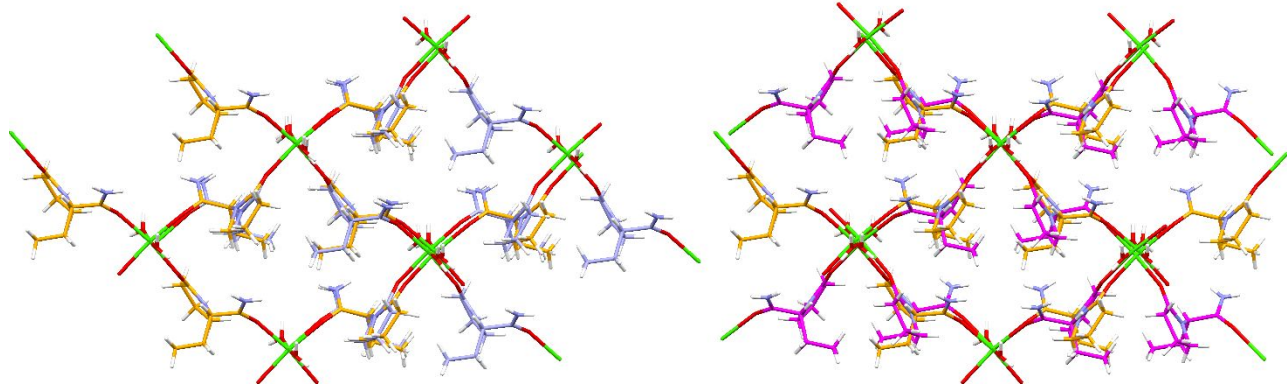


Fig. SI-1. Superposition details for $\text{LEV}_2\cdot\text{CaCl}_2\cdot 2\text{H}_2\text{O}$ and $\text{ETI}_2\cdot\text{CaCl}_2\cdot 2\text{H}_2\text{O}$. Both LEV and ETI crystallize in a C-centred unit cell with very similar unit cell parameters. Both structures show layers, where in ETI the layers contain either the R or S enantiomer. Superposition of the S-ETI layer onto the LEV layer shows a large similarity in crystal packing (Left). Superposition of the R-ETI layer onto LEV (right) reveals that the overall layer conformation is kept and that the molecules are able to adapt themselves to the local change in chirality.

Details of hydrogen bonds for cocrystals

Table S1. Hydrogen bond lengths/ \AA and angles/ $^\circ$ for $\text{LEV}_2\cdot\text{CaCl}_2\cdot 2\text{H}_2\text{O}$

D-H…A	d (D-H)	d (H…A)	d (D…A)	\angle DHA
N ₃ -H ₃ A…Cl ₁	0.86	2.47	3.310(7)	166
N ₃ -H ₃ B…Cl ₂ ⁱ	0.86	2.42	3.215(7)	154
N ₄ -H ₄ A N…Cl ₂	0.86	2.5	3.257(7)	148
O ₅ -H ₅ A…Cl ₂ ⁱⁱ	0.82	2.34	3.151(6)	169
O ₅ -H ₅ B…Cl ₁ ⁱⁱⁱ	0.82	2.33	3.143(5)	175
N ₄ -H ₄ B N…Cl ₁	0.86	2.36	3.214(7)	170
O ₆ -H ₆ A…Cl ₁	0.82	2.33	3.131(5)	165
O ₆ -H ₆ B…Cl ₂	0.82	2.39	3.138(6)	152

Symmetry codes: (i) $1/2+x, 1/2+y, z$; (ii) $1-x, y, 2-z$; (iii) $3/2-x, -1/2+y, 2-z$.

Table S2. Hydrogen bond lengths/ \AA and angles/ $^\circ$ for $\text{ETI}_2\cdot\text{CaCl}_2\cdot 2\text{H}_2\text{O}$

D-H…A	d (D-H)	d (H…A)	d (D…A)	\angle DHA
N ₂ -H ₂ A…Cl ₁ ⁱⁱ	0.77(5)	2.49(6)	3.248(5)	168(6)
N ₂ -H ₂ B…Cl ₁ ⁱⁱⁱ	0.85(6)	2.48(6)	3.317(5)	167(4)
O ₃ -H ₃ A…Cl ₁ ⁱ	0.83(3)	2.32(3)	3.145(3)	172(3)
O ₃ -H ₃ B…Cl ₁	0.82(5)	2.30(5)	3.109(3)	170(4)

Symmetry codes: (i) $1-x, -y, 1-z$; (ii) $1-x, y, 1/2-z$; (iii) $1/2+x, 1/2-y, -1/2+z$.

Table S3. Hydrogen bond lengths/ \AA and angles/ $^\circ$ for $\text{LEV}_2\cdot\text{MgCl}_2\cdot 2\text{H}_2\text{O}$

D-H…A	d (D-H)	d (H…A)	d (D…A)	\angle DHA
O ₂ -H ₂ A…Cl ₄₁ ⁱⁱⁱ	0.82	2.52	3.193(2)	140

O ₂ -H ₂ B···Cl ₄₂ ^{iv}	0.82	2.48	3.227(2)	153
N ₁₃ -H ₁₃ A···Cl ₄₂	0.89	2.35	3.186(3)	156
N ₁₃ -H ₁₃ B···Cl ₄₁	0.89	2.34	3.215(3)	170
O ₂₂ -H ₂₂ A···Cl ₄₁ ⁱ	0.82	2.33	3.148(3)	172
O ₂₂ -H ₂₂ B···Cl ₄₂ ⁱ	0.82	2.45	3.191(3)	151
N ₃₃ -H ₃₃ B···Cl ₄₂ ⁱ	0.89	2.42	3.197(14)	146
N ₃₃ -H ₃₃ C···Cl ₄₁ ⁱⁱ	0.89	2.43	3.212(14)	147

Symmetry codes: (i) x,y,1+z; (ii) -1/2+x,-1/2+y,1+z; (iii) 2-x,y,1-z ; (iv) 3/2-x,1/2+y,1-z.

Table S4. Hydrogen bond lengths/Å and angles/° for ETI₂•MgCl₂•6H₂O

D-H···A	d (D-H)	d (H···A)	d (D···A)	∠DHA
Noo9-HooA···Noo8	0.79(4)	2.42(4)	2.767(4)	108(3)
Noo9-HooA···Cl ₁ ⁱⁱⁱ	0.79(4)	2.54(4)	3.256(3)	152(4)
Noo9-HooB···Cl ₁ ⁱⁱ	0.91(4)	2.47(4)	3.375(3)	175(4)
O ₃ -H ₃ A···Cl ₁	0.74(4)	2.39(4)	3.110(3)	163(4)
O ₃ -H ₃ B···O ₂ ⁱ	0.84(4)	1.90(4)	2.738(3)	174(4)
O ₄ -H ₄ A···Cl ₁	0.77(4)	2.44(4)	3.154(3)	155(4)
O ₄ -H ₄ B···O ₅	0.96(4)	1.76(4)	2.699(4)	166(4)
O ₅ -H ₅ A···Cl ₁ ⁱⁱⁱ	0.85	2.3	3.153(4)	178
O ₅ -H ₅ B···O ₂ ^{iv}	0.85	2.01	2.845(4)	168

Symmetry codes: (i) x,y,1+z; (ii) x,y,-1+z; (iii) -x,1-y,1-z; (iv) 1-x,1-y,-z.

Table S5. Hydrogen bond lengths/Å and angles/° for ETI₂•MgCl₂•2H₂O

D-H···A	d (D-H)	d (H···A)	d (D···A)	∠DHA
N ₂ -H ₂ A···Cl ₁ ⁱ	0.86	2.54	3.284(7)	145
N ₂ -H ₂ B···Cl ₁ ⁱⁱ	0.86	2.44	3.289(7)	170
O ₃ -H ₃ A···Cl ₁	0.88	2.39	3.164(5)	147
O ₃ -H ₃ B···Cl ₁ ⁱ	0.88	2.4	3.177(5)	148

Symmetry codes: (i) 1-x,1-y,1-z; (ii) 1/2+x,1/2+y,z.

Table S6. Hydrogen bond lengths/Å and angles/° for ETI₄•MgCl₂•6H₂O

D-H···A	d (D-H)	d (H···A)	d (D···A)	∠DHA
N ₂ -H ₂ A···O ₂ ⁱ	0.86	2.06	2.919(4)	176
N ₂ -H ₂ B···Cl ₁ ⁱⁱⁱ	0.86	2.38	3.219(3)	167
N ₄ -H ₄ C···O ₄ ^{iv}	0.86	2.13	2.978(4)	169
N ₄ -H ₄ D···Cl ₁ ^v	0.86	2.42	3.252(3)	162
O ₅ -H ₅ A···O ₃	0.84(5)	1.93(5)	2.762(4)	174(4)
O ₅ -H ₅ B···O ₄ ⁱⁱ	0.77(5)	2.05(5)	2.797(3)	167(5)
O ₆ -H ₆ A···Cl ₁	0.85(4)	2.33(4)	3.145(3)	161(4)
O ₆ -H ₆ B···O ₇	0.82(6)	1.88(6)	2.697(4)	173(5)
O ₇ -H ₇ C···Cl ₁ ^v	0.85	2.48	3.266(4)	154
O ₇ -H ₇ D···O ₃	0.85	1.95	2.793(5)	173

Symmetry codes: (i) 1-x,2-y,2-z; (ii) 1-x,-y,1-z; (iii) 1-x,1-y,1-z; (iv) 2-x,-y,1-z; (v) 2-x,1-y,1-z.

Experimental XRPD vs calculated one from single crystal

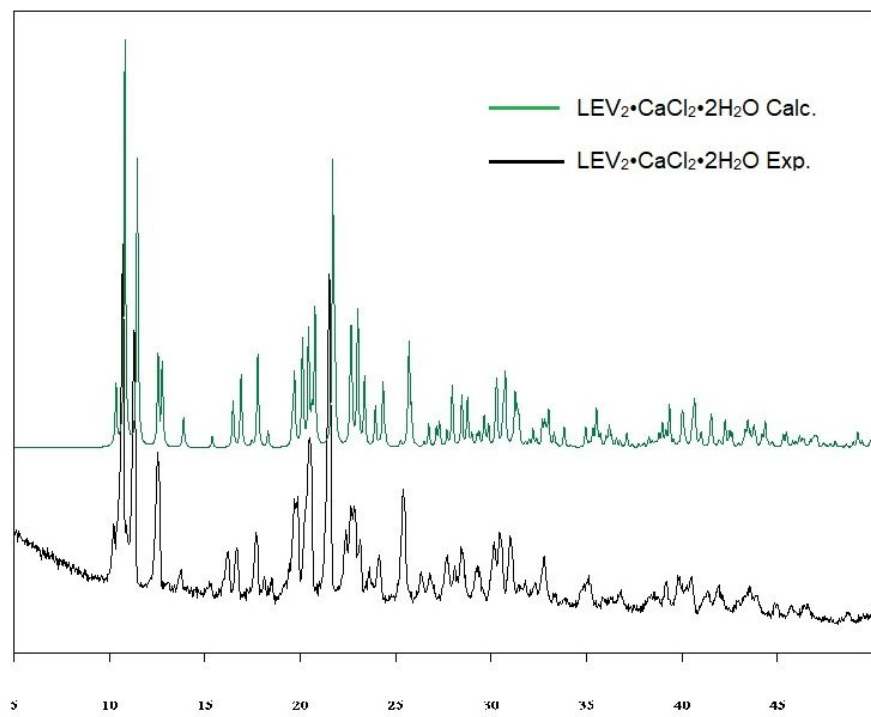


Fig. SI-2. $\text{LEV}_2\cdot\text{CaCl}_2\cdot 2\text{H}_2\text{O}$

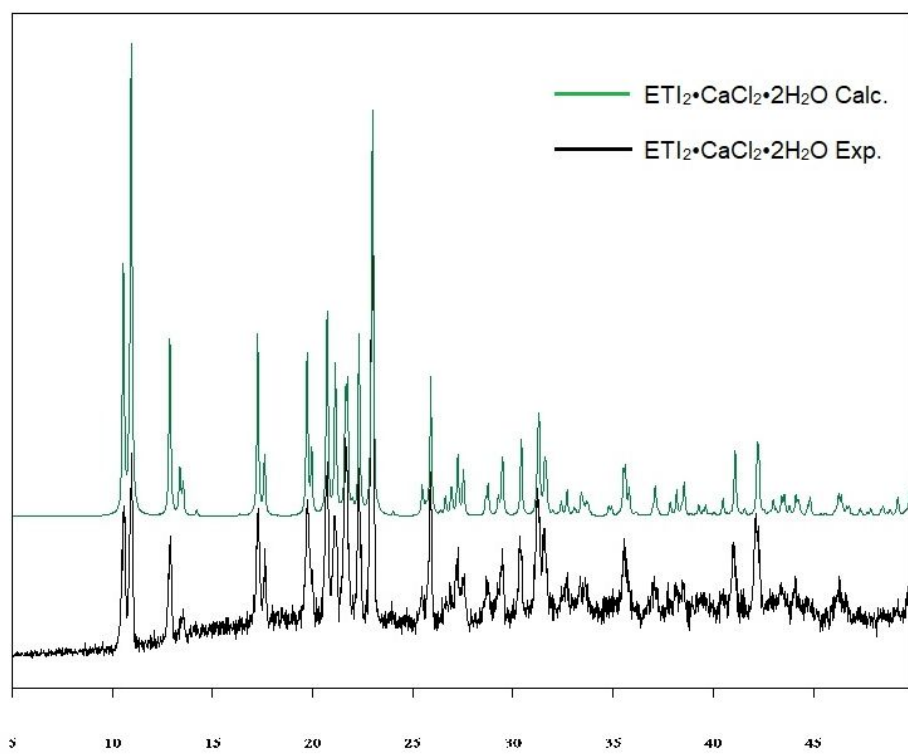


Fig. SI-3. $\text{ETI}_2\cdot\text{CaCl}_2\cdot 2\text{H}_2\text{O}$

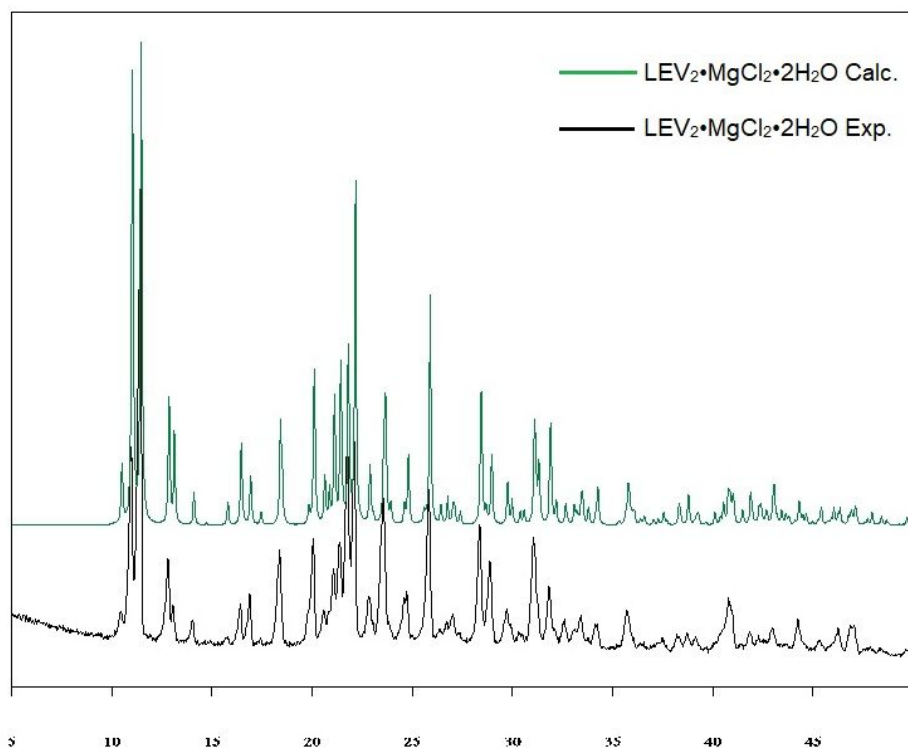


Fig. SI-4. $\text{LEV}_2 \cdot \text{MgCl}_2 \cdot 2\text{H}_2\text{O}$

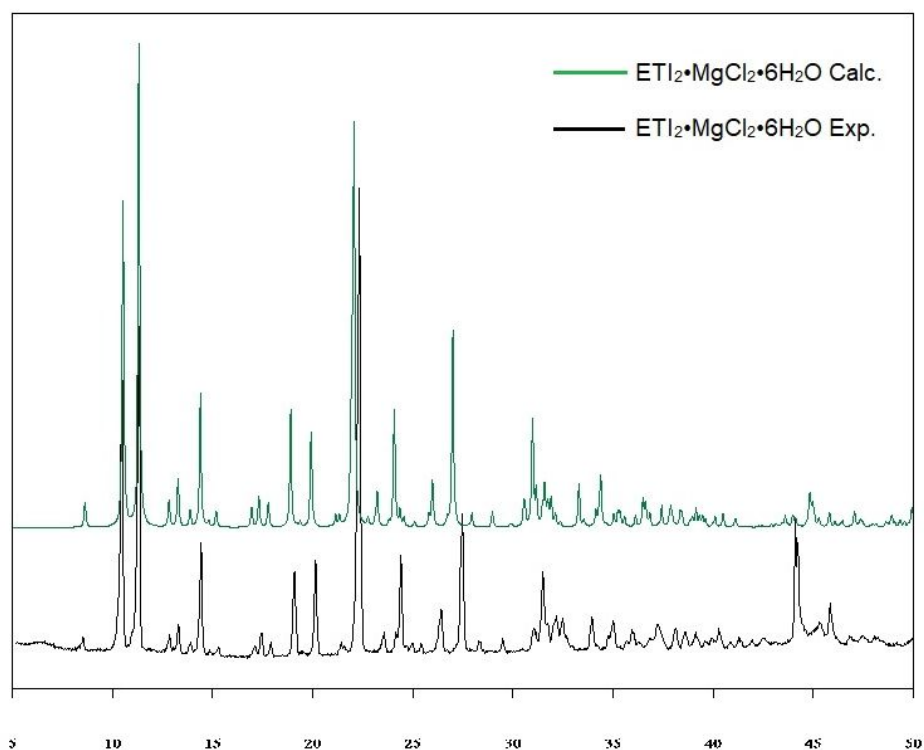


Fig. SI-5. $\text{ETI}_2 \cdot \text{MgCl}_2 \cdot 6\text{H}_2\text{O}$

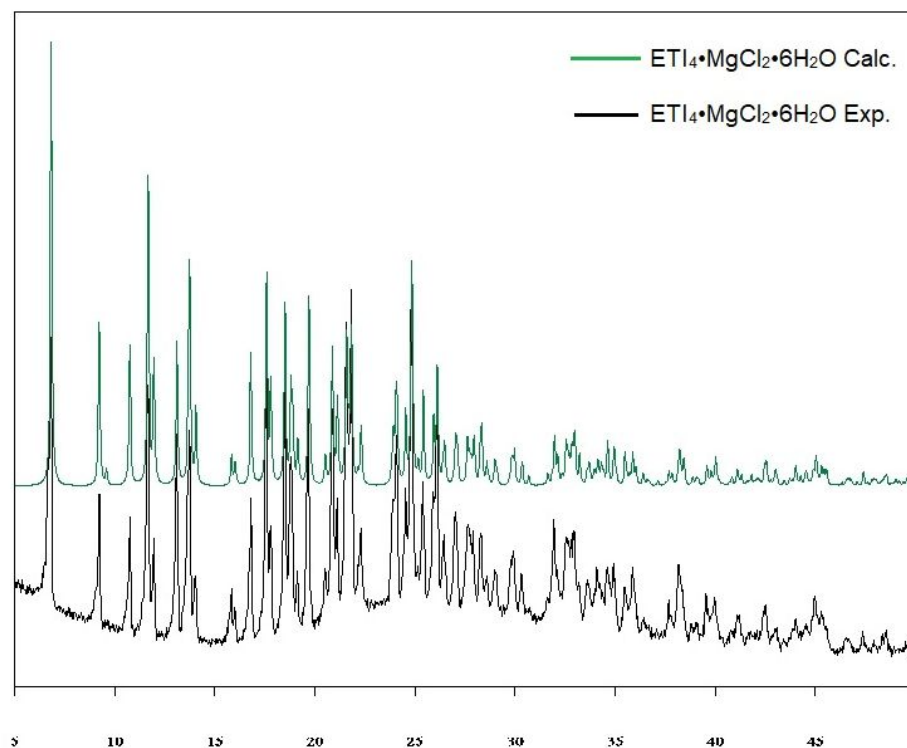


Fig. SI-6. $\text{ETI}_4 \cdot \text{MgCl}_2 \cdot 6\text{H}_2\text{O}$

DSC

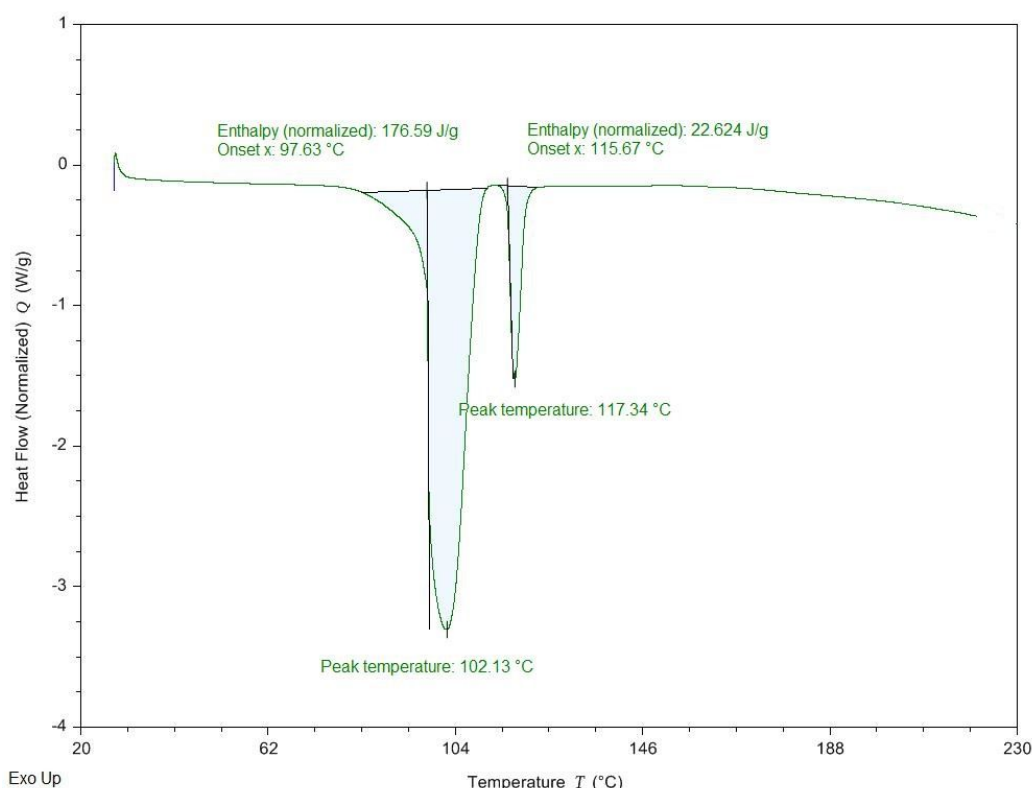


Fig. SI-7. DSC of $\text{LEV}_2 \cdot \text{CaCl}_2 \cdot 2\text{H}_2\text{O}$

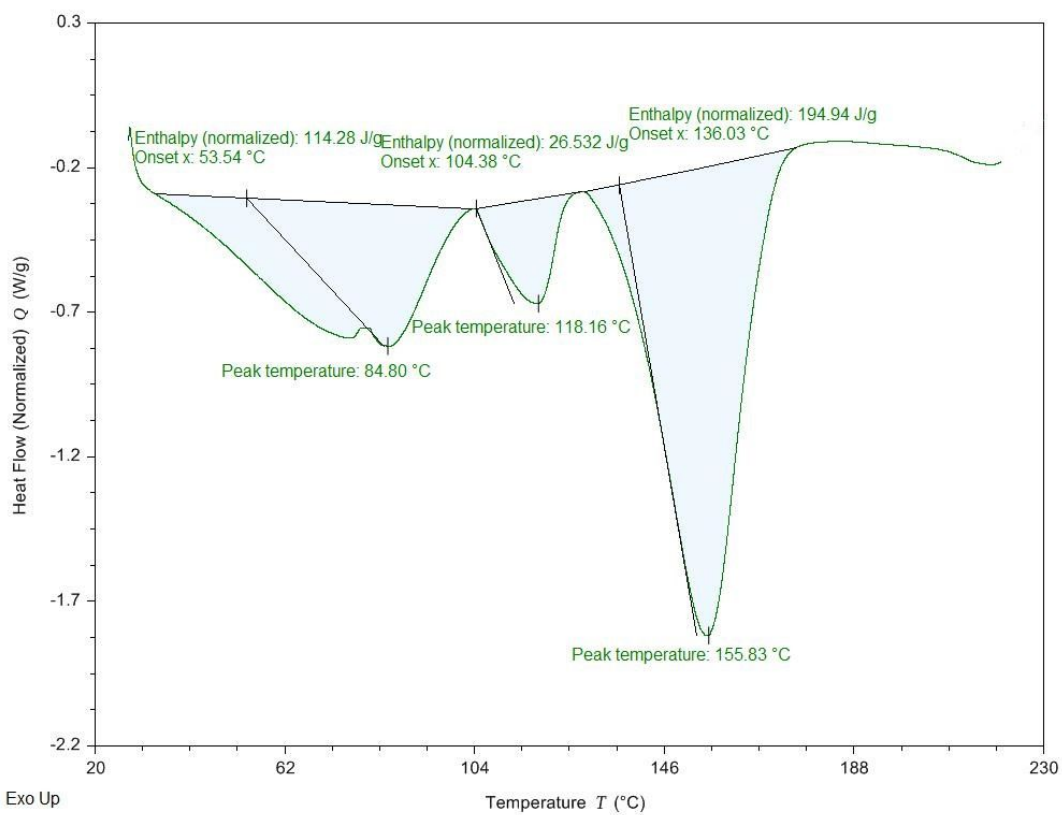


Fig SI-8. DSC of $\text{ETI}_2 \cdot \text{CaCl}_2 \cdot 2\text{H}_2\text{O}$

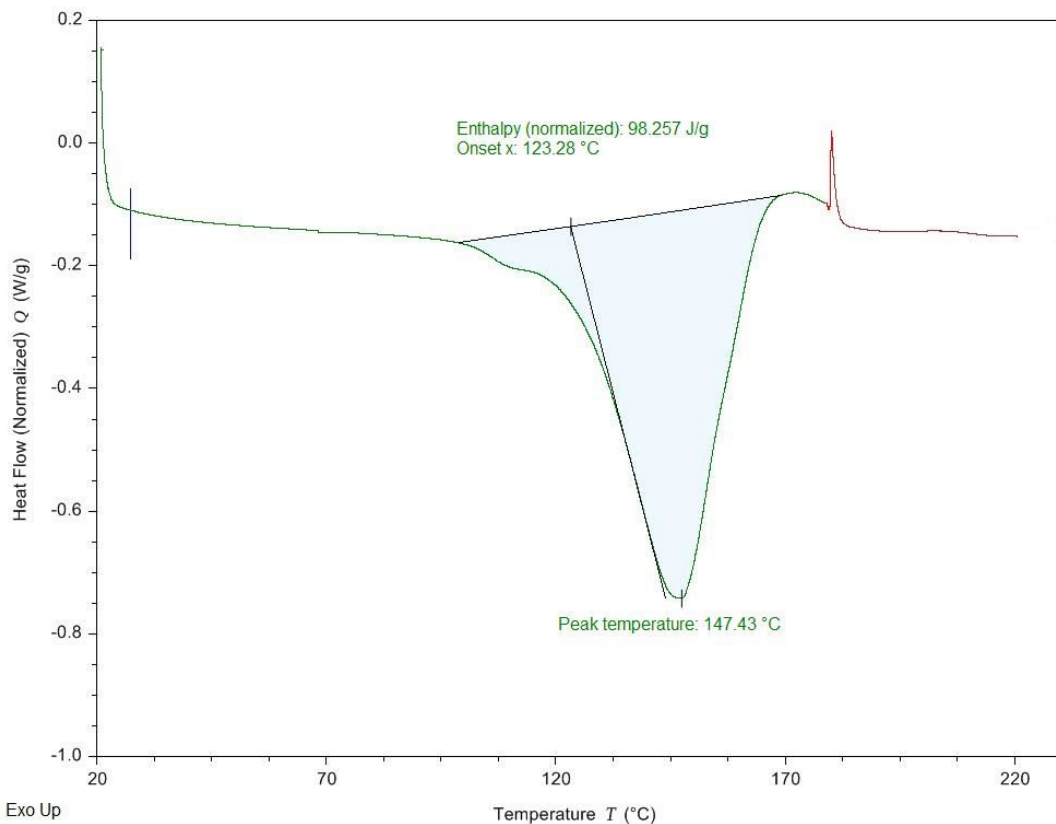


Fig. SI-9. DSC of $\text{ETI}_2 \cdot \text{CaCl}_2 \cdot 2\text{H}_2\text{O}$ (sample was kept for prolonged periods at 80 °C)

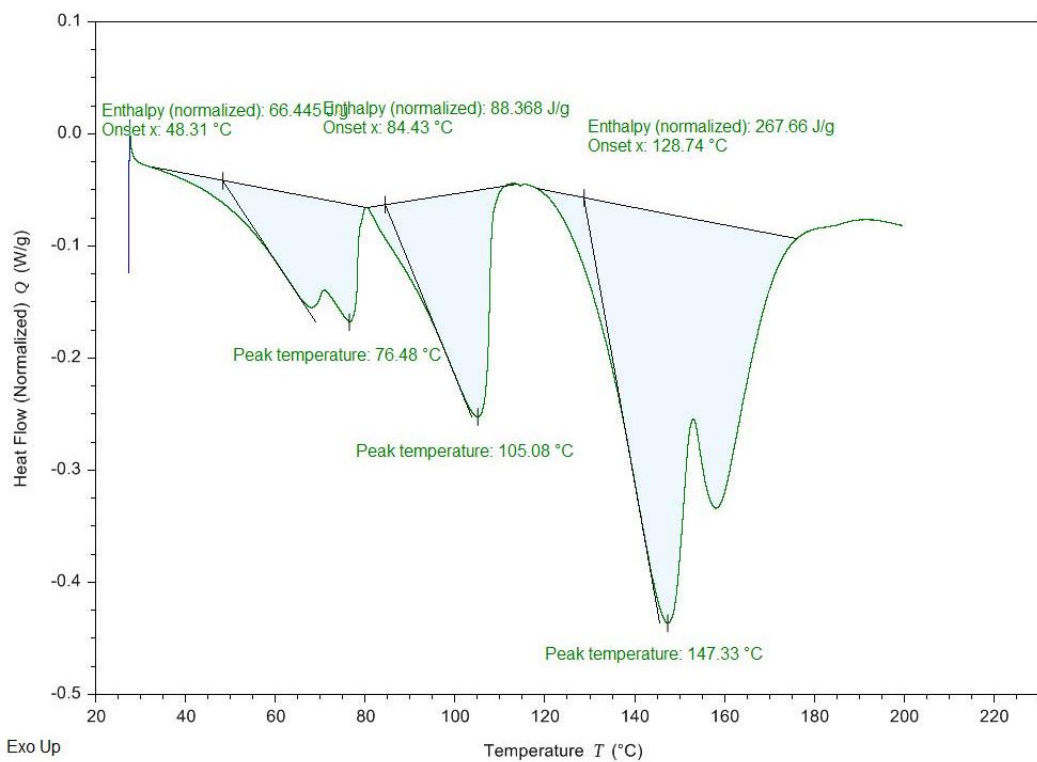


Fig. SI-10. DSC of $\text{LEV}_2\cdot\text{MgCl}_2\cdot 2\text{H}_2\text{O}$

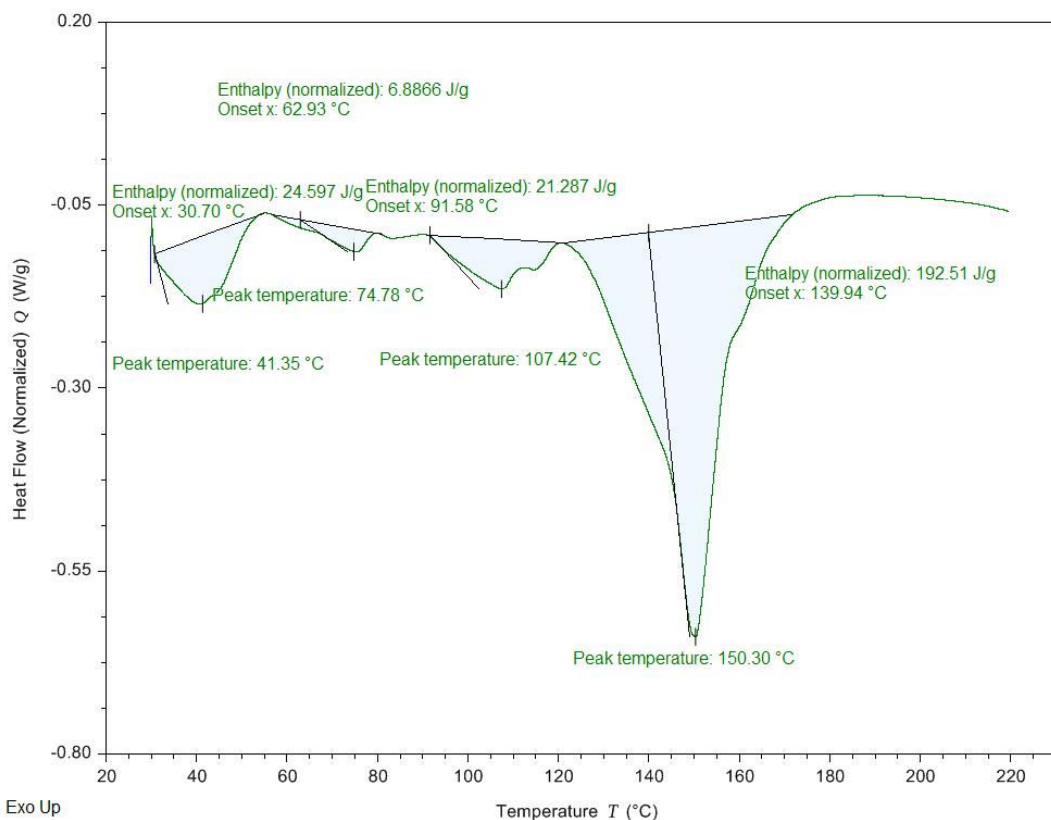


Fig. SI-11. DSC of $\text{ETI}_2\cdot\text{MgCl}_2\cdot 6\text{H}_2\text{O}$

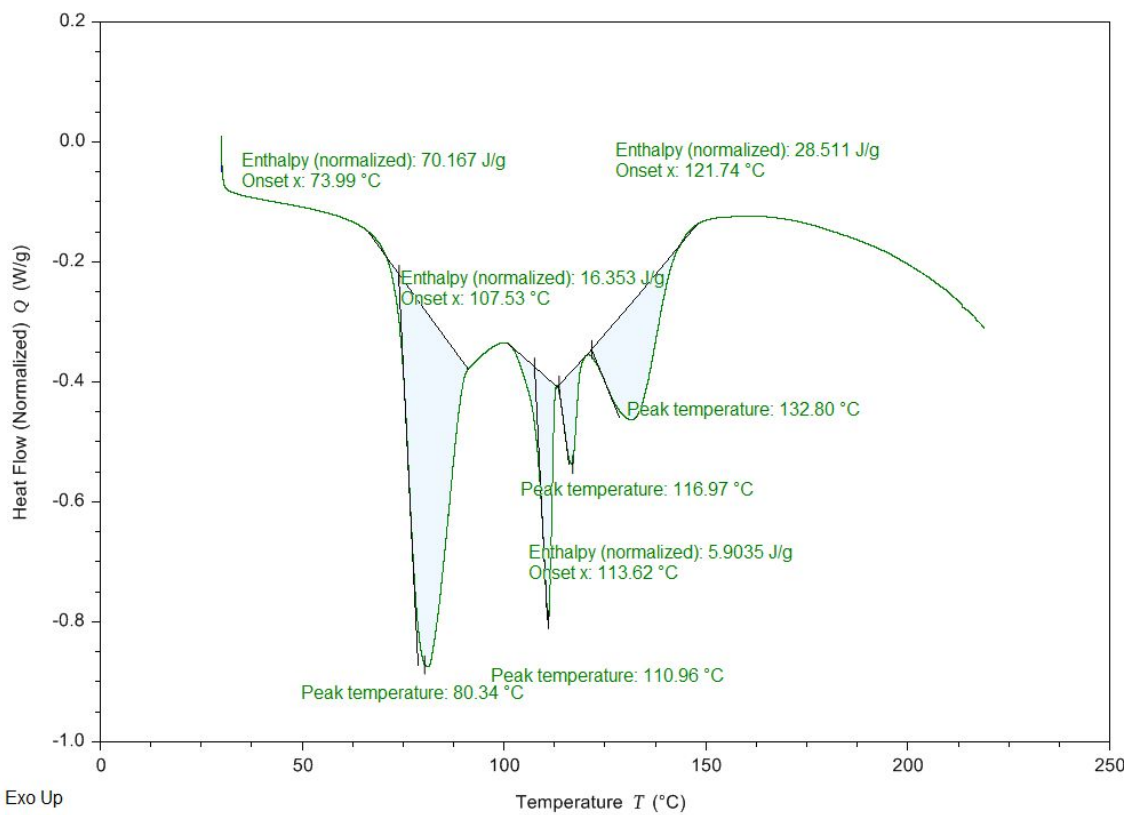


Fig. SI-12. DSC of $\text{ETI}_4 \cdot \text{MgCl}_2 \cdot 6\text{H}_2\text{O}$

VT XRPD

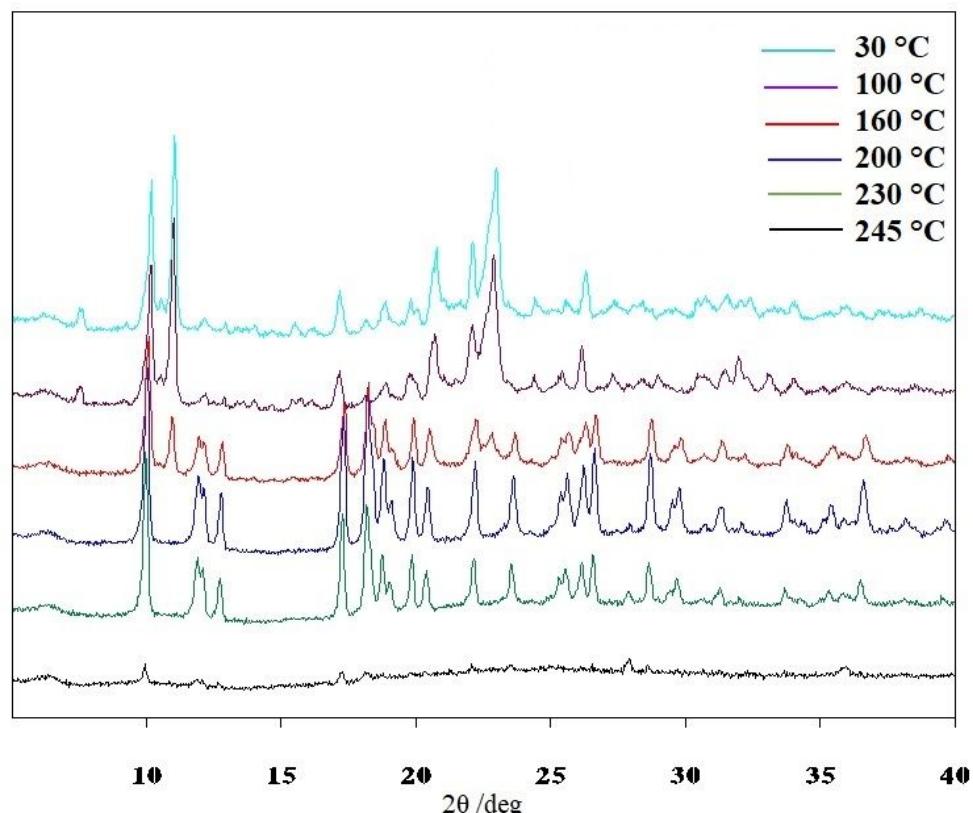


Fig. SI-13. VT XRPD of $\text{ETI}_4 \cdot \text{MgCl}_2 \cdot 4\text{H}_2\text{O}$